Part A: English Edition

Journal of Textiles and Polymers

Vol.11, No. 1, 13-26, Junuary 2023
https://doi.org/10.48302/jtp.2023.361289.1255

ORIGINAL PAPER

# Gelatin/Hydroxyapatite Porous Nanocomposite Scaffolds for Bone Tissue Engineering: Direct Mixing and Biomimetic

Marzieh Khorshidsavar, Mobina Khakbaz*, Gity Mir Mohamad Sadeghi, and Mostafa Moradi

Received: 8 September 2022, Accepted: 24 June 2023

***Abstract*- In this study, the capability of gelatin hydroxyapatite (GEL/HA) composites as organic-inorganic biological composites for use in hard tissue was investigated. These composites were made by direct mixing and biomimetic methods. In the direct mixing method, after the synthesis of hydroxyapatite, the resulting powder was mixed with gelatin; in the biomimetic method, hydroxyapatite was synthesized in the presence of gelatin. The thin layer composite substrates were prepared with a thickness of 2 mm from the resulting mixture by combining solvent casting and freeze-drying methods. These three-dimensional scaffolds were modified by glutaraldehyde (GA) as a cross-linking agent. The results showed that scaffolds have a high porosity of approximately 88% and are interconnected with holes. According to the SEM images, the average pore size is around 100 µm. Fourier transform infrared (FTIR) spectroscopy and X-ray diffraction (XRD) showed that the formation of apatite phase in non-stoichiometric form of low crystal along with extensive substitution of carbonate ions in the lattice, which is biologically very close to the apatite phase. These two composite components interact with each other not only physically, but also chemically. Compressive strength test results also showed that both scaffolds have mechanical properties similar to the cancellous bone. Young's modulus and density increased, and porosity and water absorption decreased by increasing the content of the hydroxyapatite composite. Despite the suitability of both methods, it seems that the scaffolds made by the biomimetic method are more suitable due to their higher density, higher tolerance levels of stress and Young's modulus, lower crystallinity, and replacement of carbonate ions.**

***Keywords*: gelatin, hydroxyapatite (HA), nanocomposite, porous scaffold, biomimetic**

M. Khorshidsavar
Department of Biomedical Engineering, Amirkabir University of Technology, Tehran, Iran.

M. Khakbaz, G. Mir Mohamad Sadeghi, and M. Moradi
Department of Polymer Engineering and Color Technology, Amirkabir University of Technology, Tehran, Iran.

Correspondence should be addresses to M. Khakbaz
e-mail: mkhakbaz@aut.ac.ir

## I. INTRODUCTION

Bone substitutes are often required to replace defective bone tissues due to disease, trauma, or surgery. Both autografts and allografts are used in the conventional treatment of bone defects, but there are some limitations, including donor site morbidity and a lack of donors for autografts, immunologic response and the risk of transmitting disease for allografts. For more than 50 years, various materials have been used for bone repair, including metals [1], ceramics [2,3], and synthetic and natural polymers [4-6], but these materials lack the physiological and mechanical properties of real bone.

It is noticeable that reconstruction or regeneration of organ function using tissue engineering techniques often requires temporary porous scaffolds that usually serve for directing and modulating the growth of cells that migrate from surrounding tissue or are seeded inside the porous structure of the scaffold. The scaffold must provide a suitable substrate for cell attachment, proliferation, differentiation, and migration in certain cases [7]. The basic requirements of these scaffolds are their biocompatibility, biodegradability, absorbability, expectant mechanical strength, appropriate porous structure, and easy processing for the desired shape without unwanted effects [8,9]. Up to now, many different types of scaffolds have been developed using biodegradable polymers. Among the natural biodegradable

polymers, collagen, albumin, hemoglobin, chitin, silk, chitosan, poly(lactic acid), polycaprolactone, and gelatin (GEL) are the most commonly used [10-13]. Of those mentioned, gelatin is a biodegradable polymer that exhibits excellent biocompatibility, plasticity, and adhesiveness [14]. The degree of cross-linking can control the rate of degradation. Gelatin has functional groups like carboxyl, hydroxyl, and amino that can be conjugated with ligands to produce surface modifications [15]. Therefore, in recent years, 3-dimensional porous biomimetic scaffolds have played a very important role in bone tissue engineering. Numerous biomaterials have been investigated as scaffolds for bone tissue engineering and bone repair, including natural and synthetic materials [16,17]. Although gelatin is a kind of widely used biomaterial, the disadvantage of the highly porous gelatin scaffolds is that its mechanical property is relatively weak, which limits its use for bone tissue engineering. Calcium phosphate-based materials, especially bioactive hydroxyapatite, are used as bone substitute material [18,19] due to their similarity, chemically and structurally, to the mineral portion of the bone [20]. Apatite, which resembles crystalline bone, is woven with organic fiber to create the three-dimensional composite that is natural bone. A bio-mimetic composite material with traits more akin to those of natural bone has been made by combining gelatin, a naturally occurring protein derived from collagen, the organic component of bone, with the mineral of bone (HA) [21]. The advantage of composite systems is that they combine the desired mechanical properties of both phases into one material system. Contrarily, there is growing proof that the architecture (porosity and texture) at the micron and, particularly, the nanoscale, can have a significant impact on how cells respond to materials. It is possible to make improved prostheses by controlling pore structure and surface nano-texture.

The use of polymer/ceramic composite systems as tissue engineering scaffolds for bone replacement has been the subject of numerous studies, but little attention has been paid to mechanical properties, how fabrication conditions affect pore content, and the relationship between morphology and mechanical properties [22,23].

The various kinds of polymer/ceramic composite systems such as HA/collagen [24], HA/chitosan [21], HA/collagen/poly(lactic acid) [25], HA/alginate/collagen [26], HA/gelatin [21] were employed for preparing scaffolds for tissue engineering. Due to its origins in collagen and abundance of biological functional groups, including amino acids in its backbone, which can promote cell growth and proliferation, GEL as a binding agent or matrix appears to be very appealing. The second justification is that gelatin is less expensive than collagen. The majority of bone tissue-relevant nanocomposites are based on nano-HA and a natural polymeric phase, such as nano-HA/collagen, nano-HA/gelatin, nano-HA/chitosan, and nano-HA/alginate, which were employed as tissue engineering scaffolds [21]. Two aspects of the use of HA/GEL nanocomposite scaffolds stand out: improved cell culture response and higher reinforcing quality of nano-HA particles. Research on cell proliferation on a nanocomposite scaffold showed that cells have a tendency to multiply and grow faster on materials with HA reinforcement [21]. This research aims to develop a GEL/HA-based 3-dimensional, highly porous bio-nanocomposite material. This subject was chosen as being crucial for offering systematic data on the impact of fabrication conditions.

## II. EXPERIMENTAL

### *A. Materials and Methods*

#### *A.1 Materials*

Gelatin of microbiology calcium nitrate 4-hydrate solution [$Ca(NO_3)_2.4H_2O$, 98%, Merck; No. 10305] was used for the synthesis of hydroxyapatite. Diammonium hydrogen phosphate solution [$(NH_4)_2HPO_4$, 99%, Merck; No. 1205] for the synthesis of hydroxyapatite, sodium hydroxide solution [NaOH, Merck; No. 106462] to adjust the pH and glutaraldehyde [$CH_2(CH_2CHO)_2$, 25%, Merck; No. 820603] as cross-linker were prepared.

### *B. Method of Making Porous Nanocomposite Scaffold GEL/HA*

The most appropriate and economical method for building a gelatin-based scaffold was recognized as a solvent casting technique. The building process is accelerated by this method in addition to the simplicity and easiness of using this technique. Since the used solvent is water, there would be no concern about the solvent's toxic materials' residence in the scaffold structure. In this research, the lay-up technique was used for the 3D scaffold. This technique, which is also used in various industries, is a proper method to make a 3D structure and also provide a gradient scaffold. Two techniques were used in order to build a porous nanocomposite scaffold. The first technique was a direct mixing of hydroxyapatite and gelatin powder in which the hydroxyapatite and gelatin powder were added to the distilled water container, respectively, after hydroxyapatite synthesis by the deposition method. The second technique was to synthesize hydroxyapatite powder by the deposition method but in the presence of gelatin at 37 °C and pH 10.

#### *B.1. Direct Mixing Method*

The best concentration of phosphor and calcium was used to

prepare HA. To fully dissolve the calcium nitrate in water, the first 12.0485 g weighted calcium nitrate tetrahydrate solution was added to 175 mL of distilled water and stirred for 30 min using a magnetic stirrer. In this regard, this solution was prepared by adding 4.0426 g diammonium hydrogen phosphate to 125 mL distilled water and stirred for 30 min. Then, 1 M sodium hydroxide solution changed the pH to 11.

After that, the phosphate solution was added smoothly and drop by drop to the calcium solution, which was calmly stirred with a stirrer at the pH 11 by 1 M NaOH and environment temperature. Therefore, the white sediment of HA was formed. After centrifuging the solution, it was washed with boiling water once to remove sodium according to the high solubility of sodium nitrate salt in water. After one hour of storage at -23 °C in the refrigerator, it was placed in a freeze-dryer for 24 h.

The synthesized HA powder was added to distilled water after being weighed. The gelatin powder was added after 15 min stirring and then stirred well at 37 °C for 3 h as gelatin was fully dissolved in distilled water and HA particles dispersed evenly in the gelatin solution. The gelatin concentration was kept constant for all samples (about 10%). Changing the added HA has made GEL/HA composites with 10, 20, 30, 50, and 70% hydroxyapatite. The pure gelatin sample was prepared to compare with various composites with different percentages of pure gelatin and examine the added HA. All samples were obtained under similar operations. The obtained mixture was put on a polystyrene plate after 3 h, and a full uniform compound was made and immediately put in a -4 °C refrigerator while it was at a fully smooth and balanced level. After 5 min, the gelatin in the mixture goes toward gelling by a temperature drop, and it is stiffed. The plate was transferred to a -23 °C freezer and kept for 24 h. The thin formed layer was separated from the plate and placed in a freeze-dryer. After the sublimation of its water, the porous and thin layer was obtained. The thin layer was cut in 2 mm thickness in circle form and 10 mm diameter. The obtained layer surfaces were evened by sanding and glued together using a 10% gelatin solution. The samples were floated in 1% glutaraldehyde solution on a shaker for 24 h to cross-link gelatin chains and convert it into insoluble gelatin. After 24 h, the samples were washed smoothly with distilled water three times to remove the extra and unreacted GA. Then the samples were placed in a freeze-dryer for final drying for 6 h and changed into cylinders of 12 mm height and 6 mm diameter. Therefore, the porous nanocomposite scaffold was obtained (Fig. 1).

*B.2. Biomimetic Method*

In this method, the HA is synthesized in the presence of gelatin. 10% of the gelatin was used. The calcium and phosphorus values were selected in order to obtain GEL/HA composites with 10, 30, and 50% HA by producing a desirable HA amount.

The calcium and phosphor amounts were solved in distilled water after weighting (30 min using a magnetic stirrer). The GEL was also added smoothly to the calcium solution and stirred at 37 °C for 3 h. Then, the pH of the solution reached 10 by adding 1 M NaOH solution and stirring to reach a homogeneous solution.

Since higher pH facilitates HA formation, but an alkaline solution solves more gelatin and reduces gelatin input in the composition, the phosphate solution was added to the calcium and gelatin solution drop by drop smoothly and stirred smoothly for 24 h by a stirrer, and its temperature was kept constant at 37 °C. pH was kept constant at 10 during the reaction. Adding phosphorus to calcium synthesized the HA white sediment in the gelatin container. Then it was poured into disposal polystyrene plates and quickly transferred to the refrigerator. The stiffened mixture was transferred to a -23 °C freezer by a gelling phenomenon. The thin layer was formed with 2 mm thickness, separated from the container, put on mesh, and transferred to a freeze-dryer after 24 h in order to obtain a porous scaffold. The obtained layer was cut into circles with 10 mm diameter and glued with 10% gelatin which acts as glue after smoothing by sandpaper. The cylinders were obtained at 8 and 12 mm height. These scaffolds were made in 3D by layer-up and were crosslinked by floating in 1% glutaraldehyde solution in the environment temperature and on a shaker after 24 h, and the gelatin solution changed into insoluble gelatin. After 24 h, the samples were put out

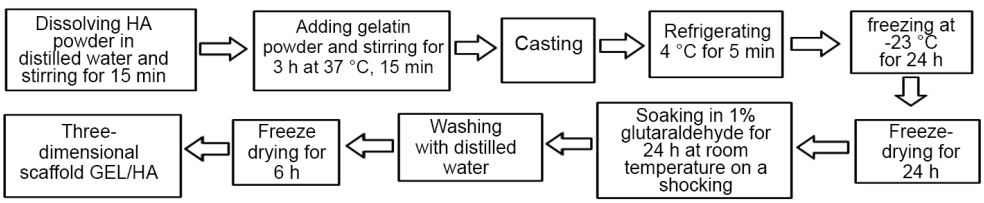


Fig. 1. Construction of three-dimensional scaffolds by direct mixing method.

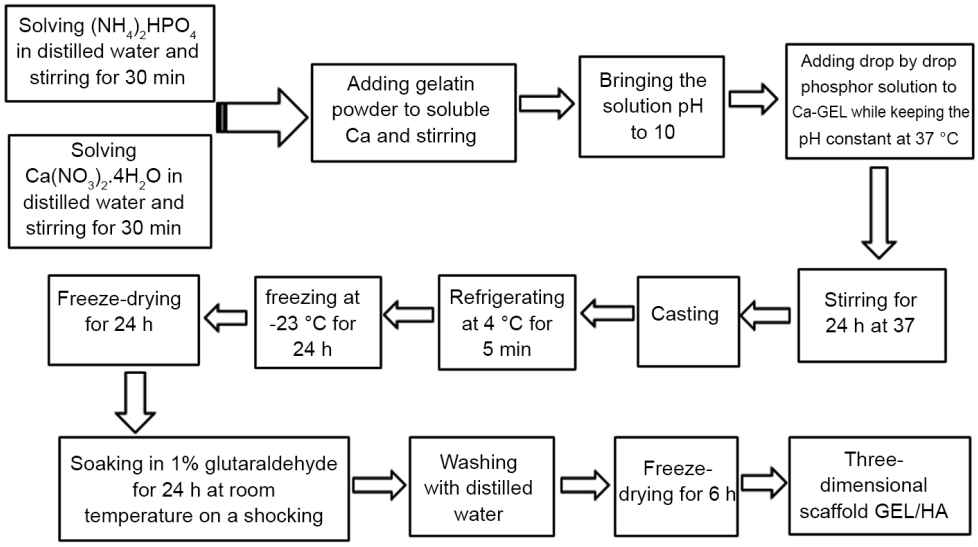


Fig. 2. Construction of three-dimensional scaffold by biomimetic method.

of the solution and washed with distilled water three times to remove the extra uncreated glutaraldehyde. The samples were fully dried and prepared for tests by a freeze-dryer for 6 h (Fig. 2).

*B.3. Determination of Porosity and Density*

According to the different percentages of hydroxyapatite in the samples, the obtained scaffolds had various porosities and densities. The density was measured by measuring the volume and mass of cylinder samples:

$$\rho = M / V \tag{1}$$

The porosity percentage will be calculated by Eq. (2):

$$\varepsilon(\%) = \left[ V_{porosity} / V_{total} \right] \times 100 \tag{2}$$

In which, $V_{porosity}$ is obtained by Eq. (3):

$$HA\rho_{gelatin} - M_{HA} / \rho - M_{gelatin} / V_{total} = V_{porosity} \tag{3}$$

The density of hydroxyapatite was considered 13.6 g/cm$^3$, and gelatin density was considered 1.35 g/cm$^3$. Five samples from each composite were prepared, and the related values to density and porosity were obtained by obtaining an average of the data.

*B.4. XRD Analysis*

The crystalline structure was obtained using X-ray diffraction patterns with XRD (D5000, Siemens, Germany) under a voltage of 30 kV and 25 mA flow. These patterns were investigated using the software Origin Pro 7.5, and the necessary data were extracted.

*C. Size of Crystallite*

The crystallite's mean sizes can be calculated using the Shearer formula.

$$T = \frac{K \times \lambda}{B \times \cos\theta_B} \tag{4}$$

T is the crystallite size, K is a constant value depending on the crystal and was considered at 89%, and λ is the irritated X wave in which the copper atom was used, so it is 1.537Å. B is the peak thickness in half of the maximum height based on radian:

$$B = (2\theta \text{ High}) - (2\theta \text{ Low})$$

In which θ is the Bragg angle (the angle of the highest peaks).

Of course, this formula is usable when the mean grain size is less than 1000Å [27].

*D. Crystallinity Percent*

The crystallinity percentage is determined by Eq. (5):

$$X_c(\%) = 1 - \left[ V_{112/300} / I_{300} \right] \times 100 \tag{5}$$

In this relation, $I_{300}$ is the height of the related peak to the surface (300), and the magnifier depth is the related peak of these two surfaces.

*E. FTIR Analysis*

In order to study the existing links in the made scaffolds, the infrared spectroscopy method with the FTIR (IFS48,

Bruker, Germany) was used.

The sample powders were prepared, and then KBr was added to be prepared for infrared spectrophotometry. the wavenumber range of measurement was between 4,000 $cm^{-1}$ to 480 $cm^{-1}$ (wavelengths 2.5 μm to 21 μm) to identify and quantify various functioning groups.

*F. Mechanical Properties of Nanocomposite Scaffolds*

The behavior of nanocomposite scaffolds containing gelatin and the power of hydroxyapatite were examined in the resistance test. The Roel Amstel apparatus performed this test in accordance with ASTM F 451-86. Scaffolds were made in the shape of cylinders with heights that are twice their diameter (12 mm height and 6mm diameter). The jaw movement speed was set at 5mm per minute according to standards. Six types of composite with different percentages of HA (0, 10, 20, 30, 50, 70) and four composites from each type were prepared (total 24 sample) and the data was calculated by averaging.

The related stress-strain curves to samples were obtained using data and drawn in MATLAB R2006a software.

*G. Water Absorption Properties*

In order to study the water absorption of the scaffolds, the buffer solution was prepared, and 50 mL buffer solution was put floating in an oven at 37 °C. The samples were taken out of the solutions in specific time intervals (the time interval was 1 h for the first day, 4 for the second day, and 10 h for the third day) and put on filter paper to go under the surface water, and then their weights were recorded. This weight is called wet weight ($W_{wet}$). These samples were taken out of the solution after three days and put in a vacuum oven at 37 °C. They were fully dried for 48 h after being removed from the oven and placed in a 40 °C environment before being weighed. The dry weight is represented as ($W_{dry}$). Therefore, the water absorption percentage of samples can be calculated by the following equation:

$$\text{Water absorption } (\%) = (W_{wet} / W_{dry} - 1) \times 100 \quad (6)$$

## III. RESULTS AND DISCUSSION

*A. Porosity and Density*

The related results are shown in Table I. The density of samples was between 0.18 and 0.53 $g/cm^3$, and their porosity percentage is between 88 and 76%. The increase in HA percentage increases density and decreases the porosity percentage (Table I). This is not only caused by the reduction of porosity and denser structure of the composite with increasing HA percentage but also related to the lower water absorption of HA compared to gelatin.

Table II shows the related results to the formed scaffolds by the biomimetic approach. It is observed that the density of samples was between 0.19 and 0.49 $g/cm^3$ and their porosity percentage was 80-88%. Here, an increase in HA percentage in the composite increases the density and decreases porosity (Table II).

The density and porosity percentage of composites

TABLE I
AMOUNTS DENSITY AND POROSITY SCAFFOLDS (GEL/HA) PREPARED BY DIRECT MIXING METHOD

| No. | Gelatin concentration in initial solution (wt%) | HA (%) | Density ($g/cm^3$) | Porosity (%) |
|---|---|---|---|---|
| 1 | 10 | 0 | 0.189±0.021 | 87.67±1.98 |
| 2 | 10 | 10 | 0.192±0.048 | 86.57±3.36 |
| 3 | 10 | 20 | 0.205±0.026 | 85.54±1.7 |
| 4 | 10 | 30 | 0.303±0.07 | 81.43±4.31 |
| 5 | 10 | 50 | 0.397±0.091 | 79.02±4.81 |
| 6 | 10 | 70 | 0.528±0.121 | 76.56±5.35 |

TABLE II
AMOUNTS OF DENSITY AND POROSITY SCAFFOLDS (GEL/HA) PREPARED BY THE BIOMIMETIC METHOD

| No. | Gelatin concentration in initial solution (wt%) | HA (%) | Density ($g/cm^3$) | Porosity (%) |
|---|---|---|---|---|
| 1 | 10 | 0 | 0.189±0.21 | 87.67±1.98 |
| 2 | 10 | 10 | 0.424±1.07 | 86.26±7.49 |
| 3 | 10 | 30 | 0.464±0.97 | 26.28±5.99 |
| 4 | 10 | 50 | 0.487±0.57 | 80.01±3.03 |

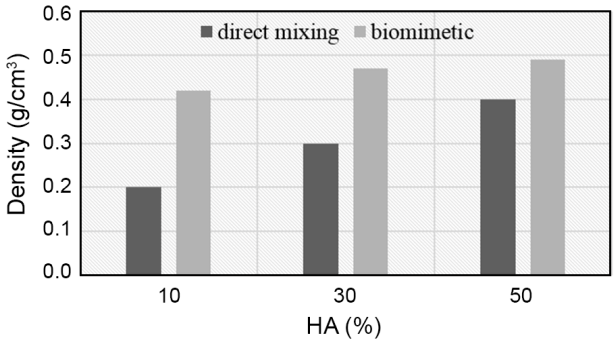


Fig. 3. Density of scaffolds made by direct mixing and biomimetic techniques.

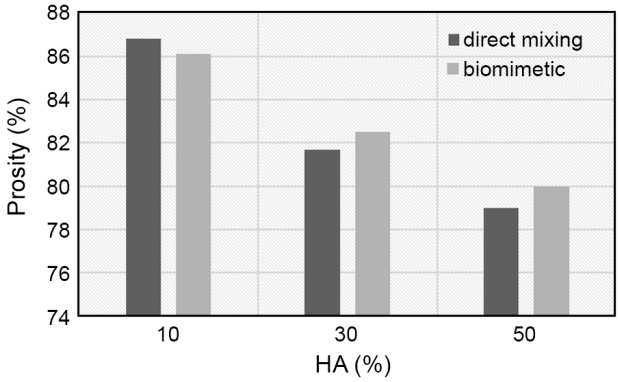


Fig. 4. Porosity percent of scaffolds made by direct mixing and biomimetic techniques.

made using the direct mixing and biomimetic techniques are compared in Figs. 3 and 4. It is observed that the density and porosity percentage of scaffolds prepared by the biomimetic technique are greater (Figs. 3 and 4).

*B. XRD Analysis*

Fig. 5 shows the diffraction patterns for the HA synthesized powder. The detected peaks confirm the fact that the synthesized powder is HA. Their smooth form was drawn by a five-point, not nine-point, Savitsky-Golay function, and the sign "*" shows related peaks to HA. This pattern can be used for the first method, that is, the direct mixing method.

The pattern shown in Fig. 6 belongs to pure gelatin. As it is observed, the pure gelatin shows intensive peaks ranging from 2θ~20°, that is, the gelatin index.

The diffraction pattern of 10 and 30% composite scaffolds made using biomimetic technique are shown in Figs. 7 and 8.

The observed peaks show that HA is present in all samples. As was expected, the XRD, GEL/HA nanocomposite-related peaks to both phases show their mean apatite, which was in 2θ~32° and in gelatin 2θ~20°. Adding CAP vividly shows the low crystalline apatite

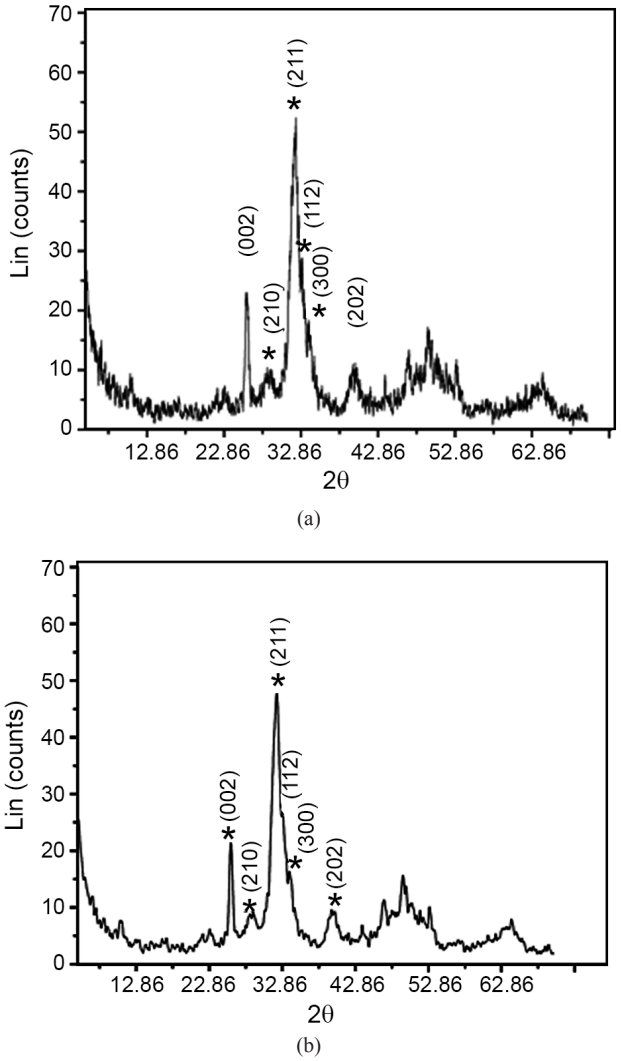


Fig. 5. XRD pattern obtained from: (a) synthesized powder HA and (b) smoothed form.

phase extension.

In the related pattern, the 30% nanocomposite was made by biomimetic technique and the peak related to sodium nitrate salt was observed before the cross-linking step (Fig. 8). This salt is the result of NaOH reaction with HA synthesis materials which remained in the compounds for

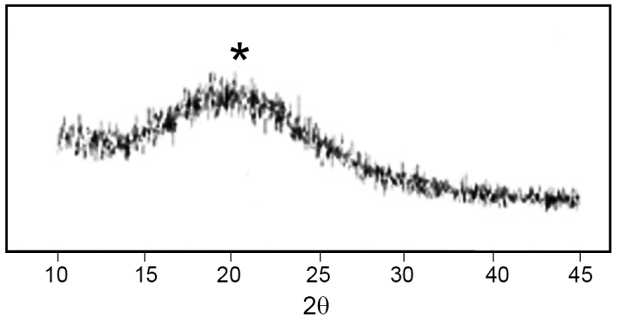


Fig. 6. XRD pattern of pure gelatin.

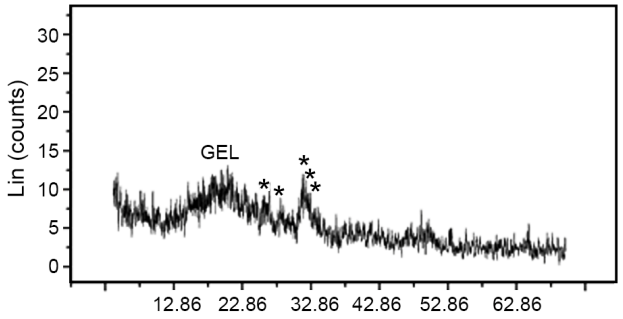


Fig. 7. XRD pattern of composite scaffolds (10%) made by biomimetic method before crosslinking.

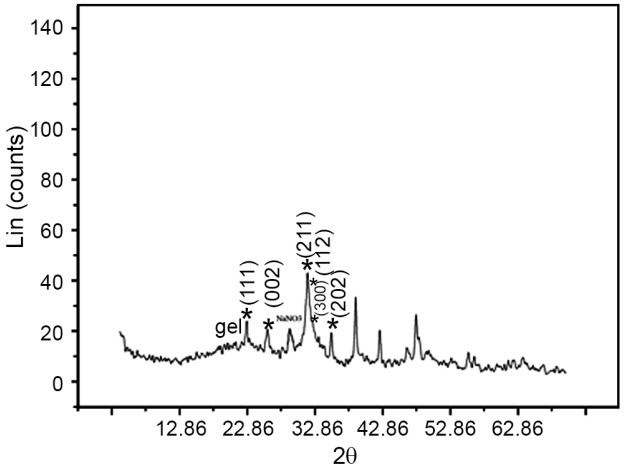


Fig. 8. XRD pattern smoothed of composite scaffolds (30%) made by biomimetic method before crosslinking.

not being centrifuged, but this scaffold stayed for 24 h in 1% HA solution. It is expected that in the scaffold, the high solubility of sodium nitrate in water will decrease after cross-linking and washing. The absence of this peak in the 10% biomimetic nanocomposite after cross-linking proves this claim. Comparing the samples made by two different methods showed that the peaks related to pages 111 and 002 of biomimetic are less than the ones in direct mixing, which show lower HA crystallinity in the composite of HA prepared by biomimetic (Fig. 9). In some references, the sharper and discrete peaks show high crystallinity for HA. In other words, the weak separation of the peaks, especially between the (211) and (112) planes, indicates the crystallinity of the apatite phase. The recent hetaeristic that is attributed to low crystallinity and very small sizes of the crystal is usually observed in an apatite crystal in the presence of an organic phase.

The results of the study by Chang, Ko, and Douglas confirmed this matter. Their study showed that two important peak intensities decreased for (211) and (002) by the gelatin content increase. This shows a decrease in the low energy for crystal growth with increasing gelatin

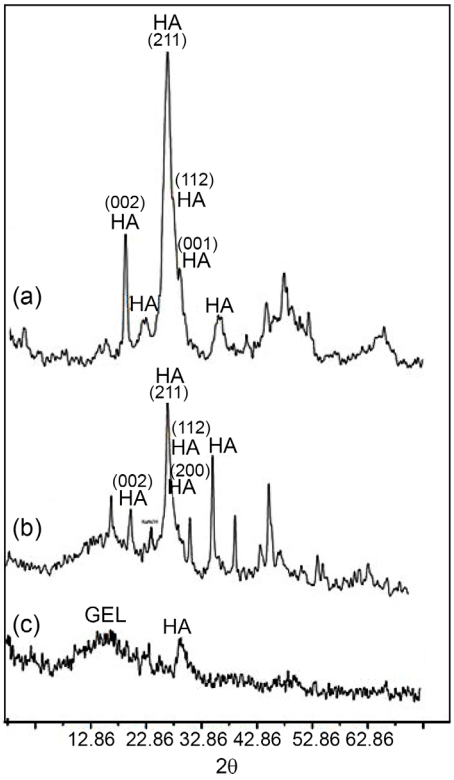


Fig. 9. Comparison of the intensity peaks of the plates (002) and (211) composite prepared: (a) powder HA, (b) 30% of biomimetic, and (c) 10% of biomimetic.

content [28].

HA with less crystallinity is closer to biological HA and moderates the destruction problem for having a higher destruction rate. On the other hand, low crystallinity of HA is very important for recasting in vivo environments and shows more alternation of the carbonate ion [29].

### *C. Size and Percentage of Crystallite*

The crystallite size of scaffold of composite 30% made by direct mixing method was estimated 7.115 nm and for that of made biomimetic method for 30 and 10% composites were 8.149 and 4.697 nm, respectively.

The crystallite sizes in 30% composites are very close to each other in direct mixing and biomimetic techniques. Of course, there is a possibility of adhesion of the particles and this increase in size can be evaluated and compared by TEM in the presence or absence and difference between particles, and agglomeration in the scaffolds formed. Scaffolds formed by the first technique adhere to each other during the mixing of HA powder with previous nano-sized HA and their size reaches microns. As expected, the size of the crystals was significantly reduced in the 10% composite compared to the 30% composite for the size of

the gelatin content relative to HA.

*D. FTIR Analysis*

Fig. 10 shows all FTIR spectrums. The pure gelatin amide bond in C=O stretching, [~1650 $cm^{-1}$], N-H deformation [~1550 $cm^{-1}$], and N-H bending [~1250 $cm^{-1}$] and carboxyl bond in 1300-1450 $cm^{-1}$ show the attributed present amino acids in the main gelatin chain such as glycine, proline, and hydroxyproline. In the FTIR spectra of GEL/HA composite, the bonds such as NH stretching at about 13431 $cm^{-1}$ for amid A, CH stretching at 2928 $cm^{-1}$ for amid B, C=O stretching to amid I at 1600-1700 $cm^{-1}$, NH bending at 1500-1550 $cm^{-1}$ for amid II and NH deformation at 1200-1300 $cm^{-1}$ for amid III can be seen. Of course, amid III is not seen in the 10% composite prepared by the direct mixing. The amid I bond is strong, amid II is weak, and amid III is medium. The presence of amid I and II bonds shows that the gelatin prepared from collagen protects the helix collagen structure even after changing its nature.

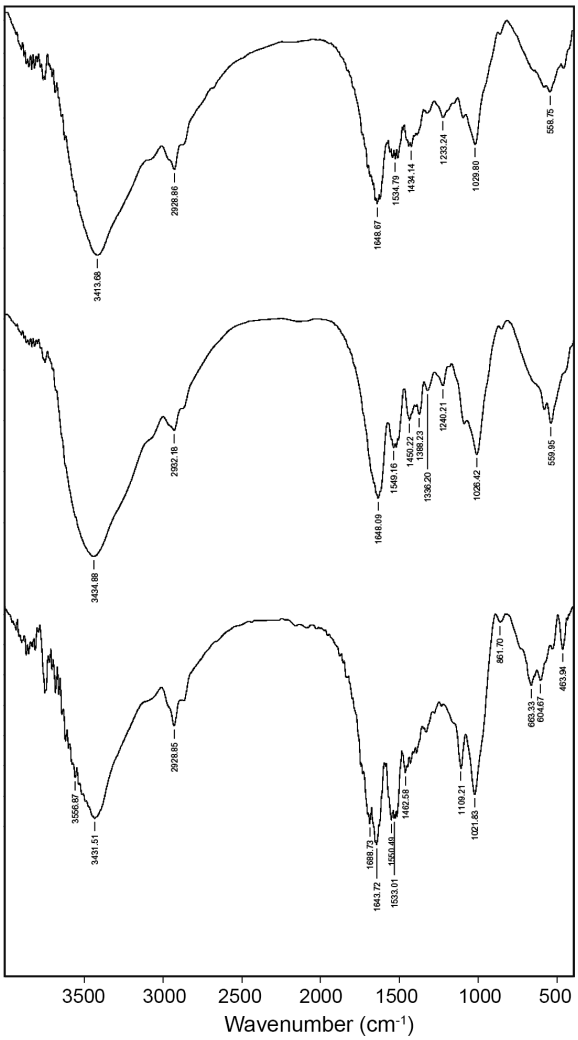


Fig. 10. FTIR spectra of HA and composites made by biomimetic (10 and 30%) and direct mixing (30%) techniques (in order from top to bottom).

Therefore, according to the phase and structural observations, it is confirmed that gelatin, even denatured gelatin, protects many biological groups [30]. In the GEL/HA composite, the apatite phase is included in the gelatin matrix by covalence interaction between $Ca^{2+}$ apatite ions and the R-COO- ion of gelatin molecules [31].

The related bonds to HA in the composite scaffolds are seen as the following:

OH- stretching [~3556 $cm^{-1}$], OH- liberational [~663 $cm^{-1}$], high $PO_4$[ν1, ν3;900-120 $cm^{-1}$] bands; and low $PO_4$[ν2, ν4 400-750 $cm^{-1}$].

In addition, the C-O bond (carbonate bond) is seen in 1350-1550 $cm^{-1}$ [υ3] and 850-890 $cm^{-1}$ [υ2] in the FTIR spectrum of the prepared composite samples. The presence of these bonds shows a high level of carbonate ($CO_3$) replacement in the HA network (instead of the phosphate group) during crystal sediment. The presence of carbonate ions indicates forming of CHA.

The popular carbonate peaks were about 870 and 880 $cm^{-1}$ that are related to CHA types B and A, respectively. The bonds that appeared at about 870 $cm^{-1}$ in all three studied composites show B-CHA in these samples. The presence of carbonate bonds in the FTIR spectrum of the samples confirms that the HA present in the composite scaffolds is low crystalline and has a structure quite similar to biological carbon apatite. One related bond to the O-H group of hydroxyapatite was seen at ~663 $cm^{-1}$, indicating that some carbonate ions were replaced in the hydroxyl position and reduced the intensity of this group. In fact, they were seen as an edge in the biomimetic nanocomposites for more extensive replacement of carbonate ions than the composites prepared by the direct mixing technique, while its intensity did not reduce in the composites prepared by the direct mixing technique.

Increasing HA in composites, for example, from 10% to 30%, shows that the bonds of HA become stronger.

Since the $PO_4^{3-}$ bond in the stoichiometry apatite appears at 1032 $cm^{-1}$, it is concluded that the prepared GEL/HA nanocomposites have a non-stoichiometry apatite.

According to strong amid bonds (amid I in 1600-1700 $cm^{-1}$ and amid II in 1500-1550 $cm^{-1}$) of the FTIR spectrum, the inorganic-organic bond between the HA phase and gelatinous matrix can be seen.

In more precise studies about the gradual movement from ~1250 $cm^{-1}$ in gelatin to 1233 $cm^{-1}$ in 10% biomimetic composite and 1240 $cm^{-1}$ in 30% biomimetic composite, the sign of chemical interaction of gelatin amino acid and phosphate and the calcium ion group is HA.

The 1339 $cm^{-1}$ bond in collagen not only shows the carboxyl group but also shows one of the existing bonds in 1260-1400 $cm^{-1}$, which is attributed to the collagen type

in the biological tissue. This bond is related to the proline lateral chain irradiation. The gelatin shows this bond in 1339 $cm^{-1}$. Carboxylic acid groups of gelatin is strongly ionic at pH>7 and ionic junction links due to the gravity to provide calcium ions. It is believed that the red shift in the GEL/HA system is reinforced by the resulting irradiation from the covalent bond with $Ca^{2+}$ ions from the HA nanocrystals. The amount of this redshift is determined by sediment conditions such as pH, temperature, concentration, and aging time. Above all, it is the gelatin content that is significantly affected [33]. This shift is seen in the studied samples of this study so that this bond appears in 30% composite by the biomimetic technique that was made for 30% at 1336 $cm^{-1}$, by the direct mixing technique for 1334 $cm^{-1}$, and for the 10% biomimetic composite at 1330 $cm^{-1}$. It is seen that this red shift in 10% biomimetic composite has the highest GEL/HA. The nanocomposite structural data of GE/HA is similar to the hydroxyapatite-natural collagen and bone matrix.

Glutaraldehyde [$OHCCH_2CH_2CH_2CHO$] has two functional groups which are able to connect to free amine groups of amino acids lysine or hydroxylysine polymerase chain peptide or amino acid lysine in gelatin-free amine groups of lysine hydroxy polymerase chain peptide in gelatin. All free amine groups of gelatin react with glutaraldehyde for 5 min. By A type amid spectrum change that shows N-H stretching mode, it can be understood that the gelatin molecular structure changes significantly as a result of cross-linking. The A type amid bond spectrum of GEL/HA nanocomposite is influenced by cross-linking of the hydrogen bond and organic content [31].

Unfortunately, the related spectrum to composites was not prepared before cross-linking. However, according to the studied literature, it was seen that the A type amid bond shifts upward after cross-linking. Upward movement of the A type amid bond results from the organic-inorganic interaction of the N-H bond at 3430 $cm^{-1}$ with HA crystals, meaning that it is $OH^-$ made at 3556 $cm^{-1}$. A GA molecular bond makes a connection among gelatin molecules so that the gap between gelatin chains inside the critical gap of the reaction is low, which is needed to rearrange the next HA crystals, and it means that a free $OH^-$ content decrease [28].

Here, it is observed that the composites prepared by the biomimetic technique is the opposite of the composites prepared by the direct mixing technique, and a peak related to $OH^-$ is not seen at 3556 $cm^{-1}$. Therefore, it can be stated that HA crystals in biomimetic crystals have a stronger arrangement.

*E. Evaluation of Porosity Structure*

The layer-up composite scaffolds technique, in addition to hydroxyapatite, changes the percentage of the porous structure. The mechanism of making pores in scaffolds was freeze-drying, and these samples were exposed to this process in the layer with a two-sided extended surface. Porosity provides a high surface to connect cells and makes enough space to transfer nutrition, enter vessels, and bone growth [5]. Nanocomposites can be porous by techniques of freezing and sublimation. The ice crystals sublimation underwater freezing temperature makes it possible to protect

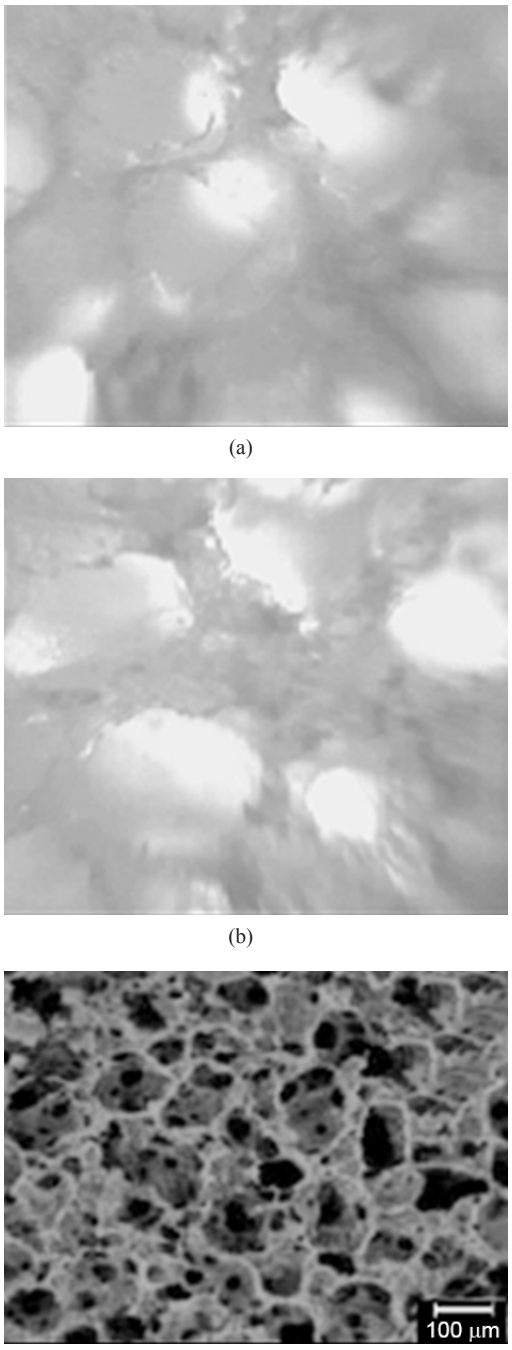


(a)

(b)

(c)

Fig. 11. Images of scaffolds surface by Optical microscope: (a) direct mixing, (b) biomimetic, and (c) SEM.

the scaffold structure from freezing. Pore form and size are directly controlled by ice crystals. The process condition was set in a low concentration of the solution (10% gelatin concentration) and high freezing temperature (-23 °C) by this method to make structures with high porosity (about 90%) and big pore size (100 μm). In addition, it is expected that sub-porosities (less than 1 μm) change by the absorbing solvent. Although the freezing and sublimation conditions are constant in this study, pore form can change by changing conditions.

The images of scaffold surfaces taken by an optical microscope revealed that the scaffolds have relatively regular porosities with related and same-size pores and separated by thin walls. According to SEM, the average pore size is 100 μm (Fig. 11).

*F. Mechanical Properties of Nanocomposite Scaffolds*

Fig. 12 shows a strain-stress diagram of a 30% nano-composite scaffold by the direct mixing technique. The first observed area is a linear area related to the elastic or reversible form in which the slope shows Young's modulus scaffold. Young's modulus was calculated based on MPa and is shown in Table III.

In the next part, which is related to plastic form change, the slope decreases and then suddenly increases (condensation area) [32]. Such behaviors in polymers are seen in systems with higher plastic form changes.

The results related to the scaffolds prepared by the direct mixing technique are shown in Table III. It is observed that the scaffolds elastic coefficient changes between 85 and 164 MPa and increases with an increase in HA% (Table III).

The flexible gelatin eventually did not break, but rather congested. Even when 50 wt% brittle HA is added, the GEL/HA composite responds to stress more effectively by absorbing energy and transmitting stress without breaking.

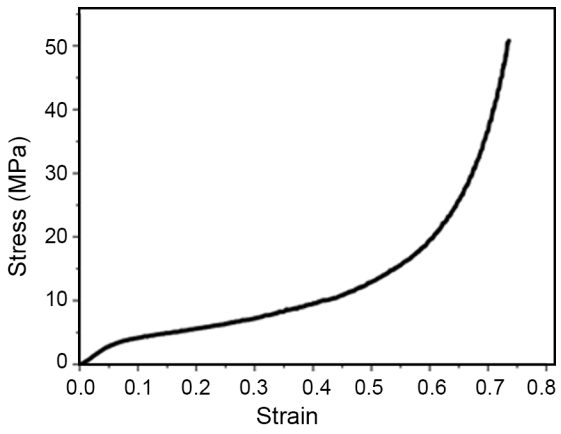


Fig. 12. Stress-strain diagram of nanocomposite (30%) scaffold by direct mixing.

TABLE III
YOUNG'S MODULUS OF GEL/HA COMPOSITE SCAFFOLDS SYNTHESIZED BY DIRECT MIXING

| No. | Gelatin concentration in initial solution (wt%) | HA (%) | Young's modulus (MPa) |
|---|---|---|---|
| 1 | 10 | 0 | 85.01±4.35 |
| 2 | 10 | 10 | 111.88±8.07 |
| 3 | 10 | 20 | 114.78±25.44 |
| 4 | 10 | 30 | 119.83±23.26 |
| 5 | 10 | 50 | 130.67±25.48 |
| 6 | 10 | 70 | 163.73±11.26 |

Such a phenomenon shows that making the HA ceramics hybrids with gelatin elements can dominate its fragility. The high flexibility of scaffold in surgery will be useful for posing scaffold in a healthy and proper manner. Above all,

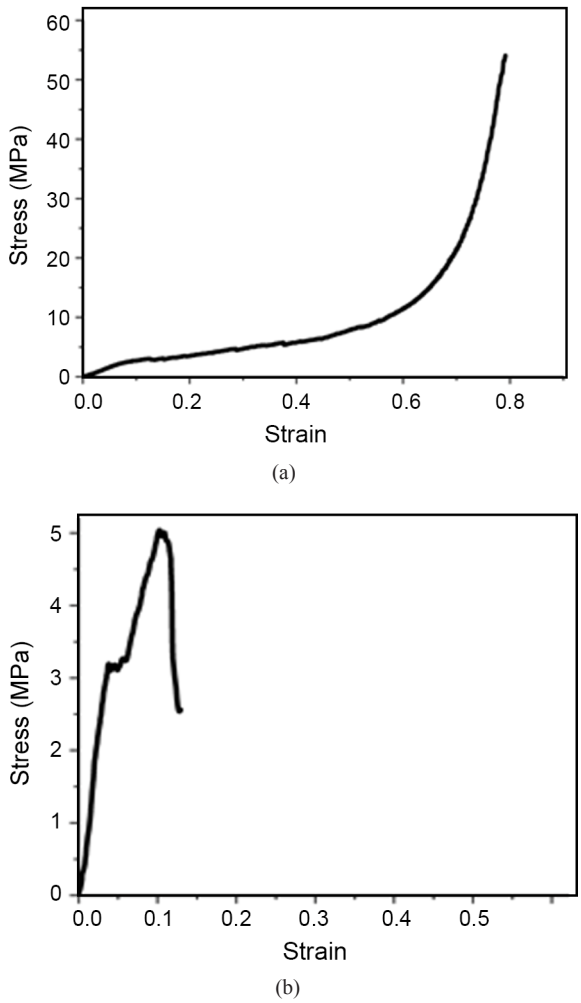


Fig. 13. Stress-strain diagram of nanocomposite scaffold by biomimetic method: (a) 10% and (b) 30%.

TABLE IV
YOUNG'S MODULUS OF GEL/HA COMPOSITE SCAFFOLDS SYNTHESIZED BY BIOMIMETIC METHOD

| No. | Gelatin concentration in initial solution (wt%) | HA (%) | Young's modulus (MPa) |
|---|---|---|---|
| 1 | 10 | 0 | 85.01±4.35 |
| 2 | 10 | 10 | 139.58±23.58 |
| 3 | 10 | 30 | 231.89±11.05 |

the stiffness of HA makes the system tolerate higher stress levels and shows a higher elastic module (slope in the first strain area <2%). In addition, about 70% of the samples were also broken.

Composites with a higher HA percentage find higher slopes in the first area of the diagram, which is the elastic deforming area. The slope that reduces in the first area belongs to plastic deforming in the next area. The composites with more HA percentage enter the condensed area sooner and tolerate higher stress for similar strain.

Fig. 13 is related to the stress strain of a scaffold prepared by the biomimetic technique. The general form of these scaffolds is similar to the ones synthesized by the direct mixing technique. However, some samples (30 and 50% composites) were broken.

The elastic coefficient was calculated for the scaffolds prepared by the biomimetic technique, as shown in Table IV.

Young's modulus of these scaffolds changes between 85 and 232 MPa and increases by an increase in HA in the composite. Young's modulus of these scaffolds is in groups of the cancellous bone [33].

The ultimate compressive pressure of the 30% composite is near the compressive strength of the cancellous bone.

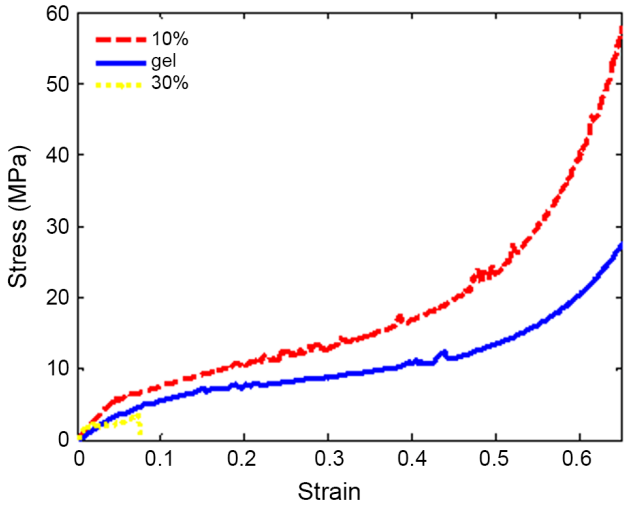


Fig. 14. Stress-strain diagram of the composite scaffold made by biomimetic method.

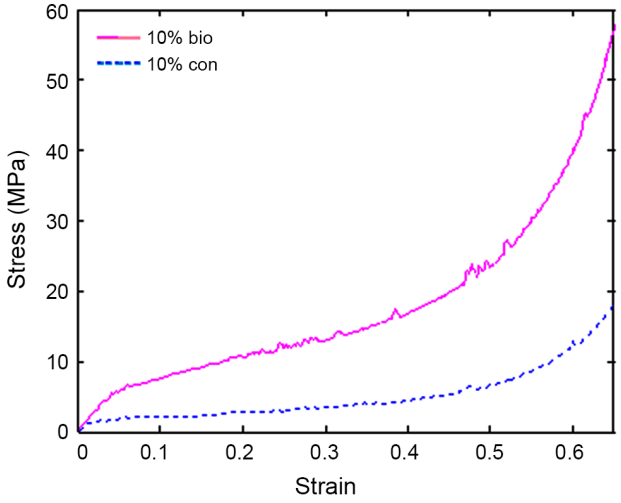


Fig. 15. Stress-strain diagram of scaffolds made by direct mixing (10%) and biomimetic (10%) technique.

Fig. 14 shows a better view of composites behaviors differences against the imposed pressure force. Increasing the HA% in the composites prepared by the biomimetic technique tolerates higher scaffold levels besides Young's modulus.

Comparing stress-strain curves for 10% scaffolds prepared by the biomimetic technique and direct mixing technique shows Young's modulus and higher stress tolerance for the biomimetic technique (Fig. 15).

By comparing the strain-stress diagram for 10% scaffolds made by biomimetic and direct mixing methods, it can be seen that Young's modulus of the prepared scaffolds is higher by the biomimetic technique. Here, Young's moduli of composites with 10 and 30% hydroxyapatite, which were made by direct mixing and biomimetic methods, have been compared. It can be seen that Young's modulus of scaffolds prepared by the biomimetic method is higher. It should also be noted that the amount and concentration of glutaraldehyde used has a significantly strong effect on the mechanical properties of the scaffold (Fig. 16).

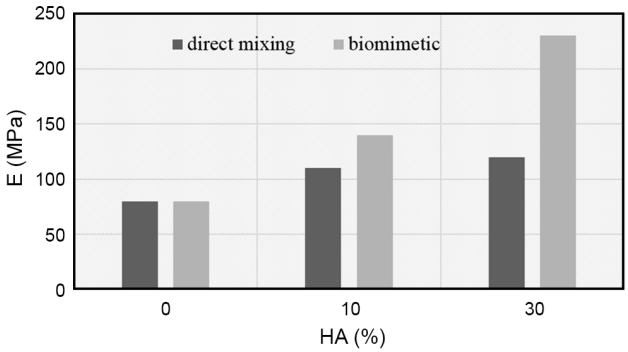


Fig. 16. Comparison of Young's modulus of scaffolds made by direct mixing and biomimetic method.

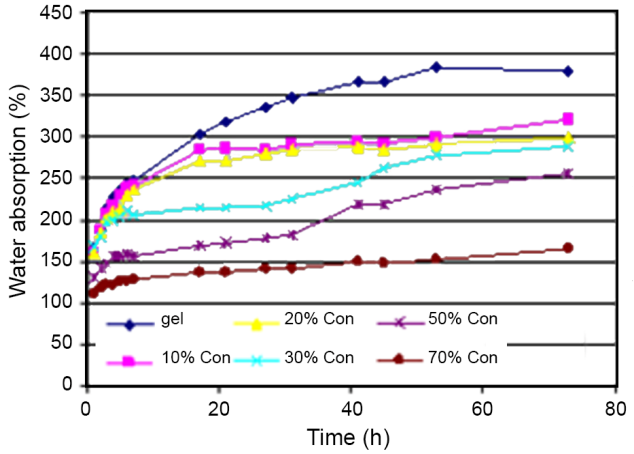


Fig. 17. Changes in percentage of water absorption of GEL/HA composite scaffolds prepared by direct mixing with time.

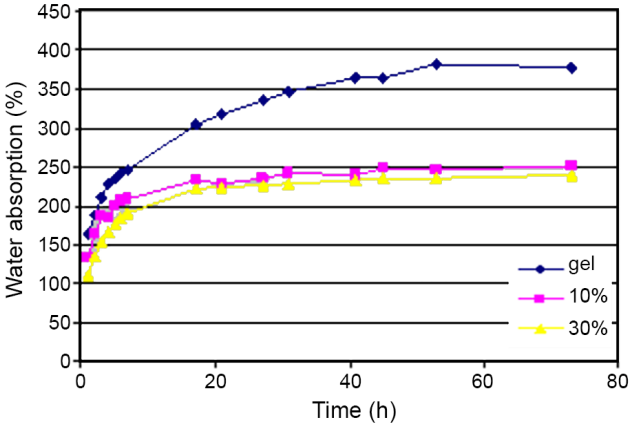


Fig. 18. Changes in percentage of water absorption of GEL/HA composite scaffolds prepared by biomimetic with time.

## IV. CONCLUSION

The method of composite materials in the development of suitable biomaterials for hard tissue, relying on the increase of structural and biological similarities to natural tissue, has attracted a lot of attention. The use of two or more components with different physicochemical properties in composite materials increases the range of application and the use of the advantages of both components, while the weak features also become less effective. In this study, the capabilities of gelatin hydroxyapatite composite as an inorganic-organic biological composite for use in hard tissue were investigated. Nanocomposites have a high porosity of approximately 88%, and the holes are interconnected. The test results of FTIR and electron diffraction spectroscopy indicated that the apatite phase formation of non-stoichiometric low crystalline along with extensive replacement of carbonate ions on the network is biologically very close to the apatite phase, and these two composite components not only physically but also chemically interact with each other. Compressive strength test results also show that both scaffolds have mechanical properties similar to cancellous bone. With increasing the content of hydroxyapatite, Young's modulus and density increased, and porosity and water absorption decreased. Despite the suitability of both methods, it seems that the scaffolds made by the biomimetic method are more appropriate due to the higher density, higher tolerance levels of stress and Young's modulus, lower crystallinity, and replacement of carbonate ions. In addition, it is observed that by increasing the gelatin content of the hydroxyapatite composites prepared by this method, the crystallinity and crystallite size, of hydroxyapatite decreased. Gelatin hydroxyapatite nanocomposite systems may make excellent scaffolds for bone tissue engineering because they closely resemble the structure of bone.

## REFERENCES

[1] J.L. González-Carrasco, "Metals as bone repair materials", In *Bone Repair Biomaterials*, Woodhead, 2009, pp. 154-193.

[2] C.H. C hang, C.Y. Lin, C.H. Chang, F.H. Liu, Y.T. Huang, and Y.S. Liao, "Enhanced biomedical applicability of $ZrO_2$–$SiO_2$ ceramic composites in 3D printed bone scaffolds", *Sci. Rep.*, vol. 12, no. 1, pp. 1-11, 2022.

[3] S. Samavedi, A.R. Whittington, and A.S. Goldstein, "Calcium phosphate ceramics in bone tissue engineering: a review of properties and their influence on cell behavior", *Acta Biomater.*, vol. 9, no. 9, pp. 8037-8045, 2013.

[4] G.R. Rodríguez, T.M.F. Patrício, and J.D. López, "Natural polymers for bone repair", In *Bone Repair Biomaterials*, Woodhead, 2019, pp. 199-232.

[5] B. Amiri, M. Ghollasi, M. Shahrousvand, M. Kamali, and A. Salimi, "Osteoblast differentiation of mesenchymal stem cells on modified PES-PEG electrospun fibrous composites loaded with $Zn_2SiO_4$ bioceramic nanoparticles", *Differentiation*, vol. 92, no. 4, pp. 148-158, 2016.

[6] P. Bhattacharjee, B. Kundu, D. Naskar, T.K. Maiti, D. Bhattacharya, and S.C. Kundu, "Nanofibrous nonmulberry silk/PVA scaffold for osteoinduction and osseointegration", *Biopolymers*, vol. 103, no. 5, pp. 271-284, 2015.

[7] R. Zeinali, L.J. Del Valle, J. Torras, and J. Puiggalí, "Recent progress on biodegradable tissue engineering scaffolds prepared by thermally-induced phase separation (Tips)", *Int. J. Mol. Sci.*, vol. 22, no. 7, pp. 3504, 2021.

[8] M.L. Chinta, A. Velidandi, N.P.P. Pabbathi, S. Dahariya, and S.R. Parcha, "Assessment of properties, applications and limitations of scaffolds based on cellulose and its derivatives for cartilage tissue engineering: A review", *Int. J. Biol. Macromol.*, vol. 175, pp. 495-515, 2021.

[9] R. Logith Kumar, A. Keshav Narayan, S. Dhivya, A. Chawla, S. Saravanan, and N. Selvamurugan, "A review of chitosan and its derivatives in bone tissue engineering", *Carbohyd. Polym.*, vol. 151, pp. 172-188, 2016.

[10] G.A.N. Atia, H.K. Shalaby, M. Zehravi, M.M. Ghobashy, H.A.N. Attia, Z. Ahmad et al., "Drug-loaded chitosan scaffolds for periodontal tissue regeneration", *Polymers*, vol. 14, no. 15, pp. 3192, 2022.

[11] A. Yıldız, A.A. Kara, and F. Acartürk, "Peptide-protein based nanofibers in pharmaceutical and biomedical applications", *Int. J. Biol. Macromol.*, vol. 148, pp. 1084-1097, 2020.

[12] T.R. de Lima Nascimento, M.M. de Amoedo Campos Velo, C.F. Silva, S. Costa Cruz, B.L.C. Gondim, R.F.L. Mondelli, and L.R.C. Castellano, "Current applications of biopolymer-based scaffolds and nanofibers as drug delivery systems", *Curr. Pharm. Design*, vol. 25, no. 37, pp. 3997-4012, 2019.

[13] A.E. Purushothaman, K. Thakur, and B. Kandasubramanian, "Development of highly porous, Electrostatic force assisted nanofiber fabrication for biological applications", *Int. J. Polym. Mater. Polym. Biomater.*, vol. 69, no. 8, pp. 477-504, 2020.

[14] H. Syed and A.K. Sailaja, "Biodegradable polymers and their applications in drug delivery system", *Interactions*, vol. 3, no. 4, 2018.

[15] M. Fernández and J. Orozco, "Advances in functionalized photosensitive polymeric nanocarriers", *Polymers*, vol. 13, no. 15, pp. 2464, 2021.

[16] S. Gundu, N. Varshney, A.K. Sahi, and S.K. Mahto, "Recent developments of biomaterial scaffolds and regenerative approaches for craniomaxillofacial bone tissue engineering", *J. Polym. Res.*, vol. 29, no. 3, pp. 1-23, 2022.

[17] S. Kanwar and S. Vijayavenkataraman, "Design of 3D printed scaffolds for bone tissue engineering: A review", *Bioprinting*, vol. 24, pp. e00167, 2021.

[18] Y. Yamaguchi, T. Matsuno, A. Miyazawa, Y. Hashimoto, and T. Satomi, "Bioactivity evaluation of biphasic hydroxyapatite bone substitutes immersed and grown with supersaturated calcium phosphate solution", *Materials*, vol. 14, no. 18, pp. 5143, 2021.

[19] R.A. Youness, M.S. Amer, and M.A. Taha, "Tribo-mechanical measurements and in vivo performance of zirconia-containing biphasic calcium phosphate material implanted in a rat model for bone replacement applications", *Mater. Chem. Phys.*, vol. 285, pp. 126085, 2022.

[20] N.N.F.N.M. Noordin, N. Ahmad, M. Mariatti, B.H. Yahaya, A.R. Sulaiman, and Z.A.A. Hamid, "A review on bioceramics scaffolds for bone defect in different types of animal models: HA and β-TCP", *Biomed. Phys. Eng. Express.*, vol. 8, no. 5, 2022.

[21] M. Azami, F. Moztarzadeh, and M. Tahriri, "Preparation, characterization and mechanical properties of controlled porous gelatin/hydroxyapatite nanocomposite through layer solvent casting combined with freeze-drying and lamination techniques", *J. Porous Mater.*, vol. 17. no. 3, pp. 313-320, 2010.

[22] J.E. Devin, M.A. Attawia, and C.T. Laurencin, "Three-dimensional degradable porous polymer-ceramic matrices for use in bone repair", *J. Biomater. Sci. Polym. Ed.*, vol. 7, no. 8, pp. 661-669, 1996.

[23] J.M. Taboas, R.D. Maddox, P.H. Krebsbach, and S.J. Hollister, "Indirect solid free form fabrication of local and global porous, biomimetic and composite 3D polymer-ceramic scaffolds", *Biomaterials*, vol. 24, no. 1, pp. 181-194, 2003.

[24] K. Grassie and Y. Khan, "Bone tissue engineering", In *Musculoskeletal Tissue Engineering*, Elsevier, 2022, pp. 1-40.

[25] B. Johari, M. Ahmadzadehzarajabad, M. Azami, M. Kazemi, M. Soleimani, S. Kargozar et al., "Repair of rat critical size calvarial defect using osteoblast-like and umbilical vein endothelial cells seeded in gelatin/hydroxyapatite scaffolds", *J. Biomed Mater. Res. Part A*, vol. 104, no. 7, pp. 1770-1778, 2016.

[26] D. Jeyachandran, L. Li, R. Fairag, L. Haglund, and M. Cerruti, "Simple fabrication and enhanced bioactivity of bioglass-poly(lactic-*co*-glycolic acid) composite scaffolds with matrix microporosity", *Macromol. Mater. Eng.*, vol. 307, no. 7, pp. 2100863, 2022.

[27] G. Cao, Nanostructures and Nanomaterials: Synthesis, Properties and Applications, Imperial college, 2004.

[28] M.C. Chang, C.C. Ko, and W.H. Douglas, "Preparation of hydroxyapatite-gelatin nanocomposite", *Biomaterials*, vol. 24, no. 17, pp. 2853-2862, 2003.

[29] E. Landi, A. Tampieri, G. Celotti, R. Langenati, M. Sandri, and S. Sprio, "Nucleation of biomimetic apatite in synthetic body fluids: dense and porous scaffold development", *Biomaterials*, vol. 26, no. 16, pp. 2835-2845, 2005.

[30] C. Shu, Y. Xianzhu, X. Zhangyin, X. Guohua, L. Hong, and Y. Kangde, "Synthesis and sintering of nanocrystalline hydroxyapatite powders by gelatin-

based precipitation method", *Ceram. Int.*, vol. 33, no. 2, pp. 193-196, 2007.

[31] W.B. Liu, S.X. Qu, R. Shen, C.X. Jiang, X.H. Li, B. Feng et al., "Influence of pH values on preparation of hydroxyapatite/gelatin composites", *J. Mater. Sci.*, vol. 41, no. 6, pp. 1851-1853, 2006.

[32] J.E. Won, A. El-Fiqi, S.H. Jegal, C.M. Han, E.J. Lee, J.C. Knowles et al., "Gelatin-apatite bone mimetic co-precipitates incorporated within biopolymer matrix to improve mechanical and biological properties useful for hard tissue repair", *J. Biomater. Appl.*, vol. 28, no. 8, pp. 1213-1225, 2014.

[33] R. Hodgskinson and J.D. Currey, "The effect of variation in structure on the Young's modulus of cancellous bone: a comparison of human and non-human material", *Proc. Inst. Mech. Eng. Part H: J. Eng. Med.*, vol. 204, no. 2, pp. 115-121, 1990.